Genome-wide approach to identify second gene targets for malignant rhabdoid tumors using high-density oligonucleotide microarrays

Junko Takita,[1] Yuyan Chen,[1] Motohiro Kato,[1,2] Kentaro Ohki,[1,3] Yusuke Sato,[4] Shigeru Ohta,[5] Kanji Sugita,[6] Riki Nishimura,[1] Noriko Hoshino,[1] Masafumi Seki,[1] Masashi Sanada,[4] Akira Oka,[1] Yasuhide Hayashi[3] and Seishi Ogawa[4]

[1]Department of Pediatrics, Graduate School of Medicine, University of Tokyo, Tokyo; [2]Cell Therapy and Transplantation Medicine, Graduate School of Medicine, University of Tokyo, Tokyo; [3]Division of Hematology/Oncology, Gunma Children's Medical Center, Gunma; [4]Department of Pathology and Tumor Biology, Graduate School of Medicine, Kyoto University, Kyoto; [5]Clinical Medicine Education Center, Shiga University of Medical Science, Shiga; [6]Department of Pediatrics, Faculty of Medicine, University of Yamanashi, Yamanashi, Japan

Malignant rhabdoid tumor (MRT) is a rare and highly lethal cancer that mainly affects infants and young children. The majority of MRT are characterized by loss of function of *SMARCB1* on chromosome 22q11.2. However, little is known about genetic changes other than *SMARCB1* alterations that are responsible for the development and/or progression of MRT. To explore additional gene targets in MRT, we analyzed 21 MRT specimens (12 fresh tumors and 9 MRT-derived cell lines) using high-density single nucleotide polymorphism genotyping microarrays. Although MRT genomes are characterized by common 22q11.2 deletions, affecting the *SMARCB1* locus with a frequency of 95.2% (20/21 specimens), other genetic changes have been less frequent. Of the 20 specimens with deletions of 22q11.2, eight specimens showed uniparental disomy of the *SMARCB1* locus with homozygous deletions or gene mutations. High-resolution analysis also disclosed the recurrent hemizygous/homozygous deletions of 7q35–q36.1, involving the *CNTNAP2* locus in three specimens. Mutations analysis of *CNTNAP2* showed a novel R157C missense mutation in a primary case, and methylation analysis showed recurrent hypermethylation of *CNTNAP2* in three of nine cell lines. These results demonstrated that *CNTNAP2* is one of the additional gene targets, other than *SMARCB1*, in MRT.

M alignant rhabdoid tumor (MRT) is an extremely rare and highly aggressive neoplasm that typically develops in infancy or early childhood.[1] Although initially described as being rhabdomyosarcomatous, an aggressive type of kidney tumor,[1] subsequent studies have revealed that MRT occurs in various sites, including the central nervous system (CNS), lung, liver, skin, and soft tissues.[2] The most frequent location of the tumor is the kidneys, followed by the CNS, and tumors originating from the latter site are referred to as atypical teratoid/rhabdoid tumors (AT/RT).[3] Cytogenetic and molecular analyses of MRT have shown recurrent deletions at 22q11.2, which resulted in identification of *SMARCB1* (OMIN 601607) as a characteristic gene abnormality of this tumor.[4] Germ-line and somatic mutations/deletions of *SMARCB1* have been reported in AT/RT as well as in epithelioid sarcoma, familial schwannomatosis, and renal medullary carcinoma.[5–8] The *SMARCB1* gene is a member of the ATP-dependent SWI/SNF chromatin-remodeling complex and is recruited to promoters of genes that regulate cell cycle, growth, and differentiation.[4] In MRT, *SMARCB1* appears to function as a classic tumor suppressor gene, such that germ-line mutations and deletions

predispose to the development of these malignancies; somatic loss or mutation of the other allele constitutes the second hit.

In recent years, genome-wide copy number analysis using single nucleotide polymorphism (SNP) arrays (SNP-chip) has been shown to have outstanding power to reveal detailed profiles of genomic abnormalities and identify new genetic targets in various cancers.[9] A previous report showed that high-resolution SNP-chip analysis could detect bi-allelic alterations in *SMARCB1* in almost all MRT cases, which suggests that *SMARCB1* is the primary mutational gene target responsible for the development of MRT and provided further evidence for the clinical utility of molecular diagnostic testing.[10] However, some MRT cases retain expression of the protein, and a small number of familial MRTs have been reported to not be associated with *SMARCB1* inactivation.[11] These findings suggest the possibility of additional relevant genetic loci distinct from *SMARCB1*. However, the detailed genetic abnormalities in MRT other than chromosome 22 have not been fully understood. Therefore, to clarify the additional genetic lesions involved in the pathogenesis of MRTs, we carried out SNP-chip analysis of 21 MRT samples.

Materials and Methods

Specimens. This study was approved by the ethics board of the University of Tokyo (Tokyo, Japan) (Approval Number 1598). Primary tumor specimens were obtained at the time of the initial surgery or biopsy from patients who were diagnosed as having MRT or AT/RT at collaborating hospitals. In total, 12 primary MRT specimens (four samples of AT/RT) and 9 cell lines derived from patients with MRT (KYM-1, TM87-16, TTC-1240, TTC-549, TTC-642, TTN-45, YAMRT, RTK(J)-4N, and STM-91-01) were analyzed in this study. The original tumor sites of the primary and cell-line specimens are described in Table S1. The TTC series and STM-91-01 were established from MRT patients. KYM-1, YAMRT, TTN-45, TM87-16, and RTK(J)-4N were generous gifts from Dr. Inoue (St. Jude Children's Research Hospital, Memphis, TN, USA), Dr. Kanegane (Toyama University, Toyama, Japan), Dr. Shimada (Children's Hospital Los Angeles), and Dr. Yokomori (Graduate School of Medicine, University of Tokyo). A neuroblastoma cell line, SJNB-1, was used as a control in the methylation analysis. All cell lines were cultured in RPMI-1640 (Gibco, Gaithersburg, MD, USA) supplemented with 9% FBS.[12]

Microarray analysis. High molecular weight DNA was isolated from tumor specimens and subjected to SNP-chip analysis using Affymetrix GeneChip Mapping 50K and/or 250K arrays (Affymetrix, Santa Clara, CA, USA), according to the manufacturer's protocol (Table S1). After appropriate normalization of mean array intensities, signal ratios between tumor and normal cells were calculated, and allele-specific copy numbers were inferred from the observed signal ratios based on the hidden Markov model using CNAG/AsCNAR software (http://www.genome.umin.jp/CNAG_DLpage/CNAG_top.html).[9] Chromosomal losses detected by SNP-chip analysis were confirmed by quantitative genomic PCR (Q-genomic PCR) for *CNTNAP2*, *LRP1B*, *FHIT*, *ROBO1*, *AUTS2*, *PTPRD*, and *ATBF1* loci.[13] *GAPDH* was used as control. Primer sets for Q-genomic PCR are listed in Table S2.

Mutation and expression analyses of *SMARCB1* and *CNTNAP2*. Direct sequencing analyses of all coding exons of *SMARCB1* and *CNTNAP2* were carried out in all samples as previously described.[14] The primer sequences and conditions of PCR for mutation analyses of these genes have been described in previous papers.[14,15] Total RNA was extracted from the nine cell lines using Isogen reagent (Nippon Gene, Osaka, Japan), according to the manufacturer's instructions and subjected to RT-PCR to synthesize cDNA using the SuperScript Preamplification System for first-strand cDNA synthesis (Life Technologies, Rockville, MD, USA). Semiquantitative RT-PCR analysis for *CNTNAP2* expression was carried out as previously described.[16]

Methylation-specific PCR and 5-aza-2-deoxycytidine treatment. Bisulfate modification of genomic DNA was carried out as previously described.[17] For methylation-specific PCR, approximately 10 ng bisulfite-treated DNA was amplified with primers for both the methylated and unmethylated sequences.[17] The primer sets for promoter region *CNTNAP2* were as described previously,[18] and the primer sets for *SMARCB1* were as follows: SMARCB1F2, 5′-gtcygtgagaagtcc tctac-3′; SMARCB1R2, 5′-gaaatcccaggtcratgagg-3′. Reaction products were separated by electrophoresis on a 2.0% agarose gel. 5-Aza-2-deoxycytidine (Sigma Chemical, Perth, WA, Australia) was dissolved in cold RPMI-1640 immediately before use. Cells were exposed to 0.5 and 1.0 mM 5-aza-2-deoxycytidine for 3 days, with the medium and drug being replaced every 24 h.[19] Cells were then harvested and used for RT-PCR analysis.

Histopathology and immunohistochemistry. For light microscopy, tumors from MRT patients were fixed in 10% buffered formalin and embedded in paraffin. Sections from the paraffin-embedded blocks were evaluated by H&E staining and immunoperoxidase techniques using a panel of mAbs, including epithelial membrane antigen, vimentin, a muscle actin-specific monoclonal antibody (HHF35), myoglobin, S100 protein, neuron-specific enolase, and SMARCB1/INI1.[14,20]

Results

Chromosome 22q11.2 deletions and mutations of *SMARCB1*. The SNP-chip analysis was carried out for 21 MRT specimens, including 12 fresh tumors and 9 cell lines, using Affymetrix GeneChip 50K *Xba*I/*Hin*dIII and/or 250K *Nsp*I/*Sty*I mapping arrays (Table S1). Although many specimens had no matched control DNA and suffered from varying degrees of normal cell contamination, the allelic compositions were accurately determined in most specimens using our CNAG/AsCNAR programs (Fig. 1a). In our SNP-chip analysis, the most frequent copy number change detected in MRT was deletion of chromosome 22q11.2 (Fig. 1a,b). In total, 20 of 21 specimens (95.2%) had LOH or homozygous deletions at 22q11.2 involving the *SMARCB1* locus (Fig. 1a,b). In eight samples, uniparental disomy (UPD) of 22q segments caused homozygous mutations/deletions of *SMARCB1* (Fig. 1b). Ten samples had homozygous focal deletions commonly involving a 175-kb region (ch22:22,353,181-22,528,353), which exclusively included *SMARCB1*. Subsequent mutation analysis revealed that five samples with heterozygous deletion or UPD at the 22q11.2 locus had mutations in *SMARCB1* (Table 1). An MRT-derived cell line with 22qUPD (YAMRT) harbored a small deletion involving exons 1–3, which was not detectable by SNP-chip analysis. In our cohort, two specimens showed hemizygous deletion at the *SMARCB1* locus, and one case showed no genetic changes within this locus. Immunohistochemical analyses of these three cases showed positive results for vimentin but negative findings for muscle lineage markers and SMARCB1, supporting the diagnosis of MRT or AT/RT. Thus, to investigate whether abnormal methylation is associated with inactivation of *SMARCB1*, bisulfate sequencing for the promoter region of *SMARCB1* was carried out in these three cases. As shown in Figure 1(c), two cases having hemizygous deletions at the *SMARCB1* locus displayed complete methylation of the CpG island. However, one case without any genetic abnormality of the *SMARCB1* locus lacked PCR products (both methylated and unmethylated) for the promoter region (Fig. 1c), suggesting that this case may harbor a small deletion involving the promoter region of *SMARCB1*, which escaped SNP array detection. In total, 20 of the 21 MRT samples had biallelic aberrations of *SMARCB1*, indicating genetic homogeneity of MRT. Molecular allelokaryotyping profiles were essentially similar between cell lines and primary tumors, providing some rationale for the combined analysis of both specimens in this study (Fig. 1b).

Other copy number changes detected in MRT. Although recurrent copy number changes other than 22q11.2 deletions were less frequent in MRT (Fig. 1a), seven loci of gains and eight loci of losses were commonly detected in multiple samples (Table 2). Importantly, some of the regions contained potential gene targets that were known to be associated with tumorigenesis of other cancers, such as *CCNL1*, *POT1*, *CNTNAP2*, and
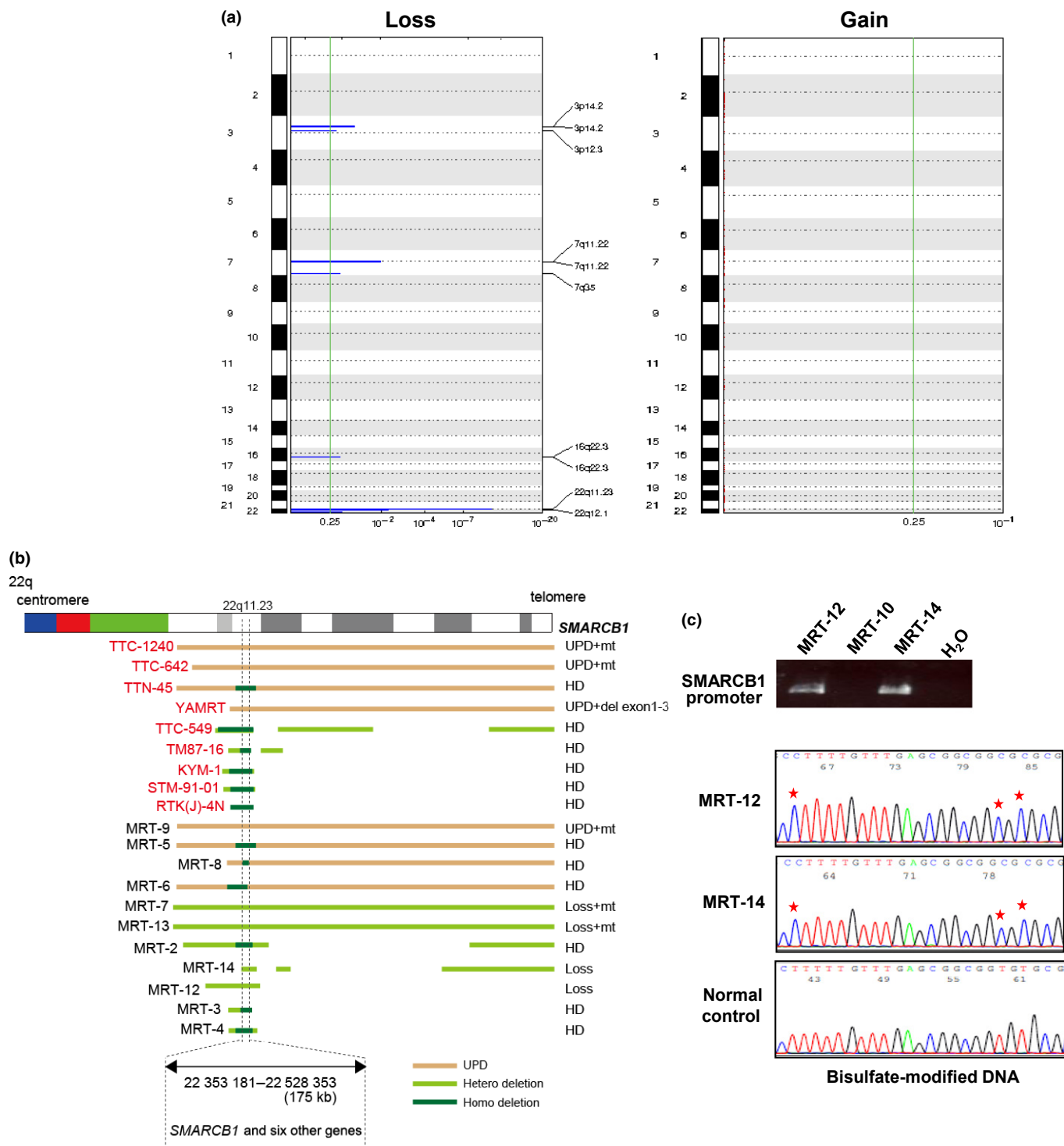
Fig. 1. Copy number changes detected in malignant rhabdoid tumors (MRT). (a) Characteristics of copy number alterations in MRT. Regions showing statistically significant increase or decrease in genomic copy number were detected using the genomic identification of significant targets in cancer (GISTIC) algorithm based on single nucleotide polymorphism array analysis. Because we did not detect any significant chromosomal gains in our cohort, nothing is shown in the right-hand figure. (b) Overall representation of aberrations of chromosome 22q11.2 in MRT. Specimens indicated by red are cell lines. Pink bar indicates uniparental disomy, and yellow and green bars indicate heterozygous deletion and homozygous deletion, respectively. The minimum overlapping deleted region was 175 kb in chromosome 22q11.2, including *SMARCB1* and another six genes. *SMARCB1* status is indicated at the right. MRT-12 and MRT-14 show heterozygous deletion of the *SMARCB1* locus, and the wild-type allele of *SMARCB1* was retained in each case. del, deletion; HD, homozygous deletion; mt, mutation; UPD, uniparental disomy. (c) Bisulfate modification- and methylation-specific PCR for *SMARCB1* in fresh tumors without biallelic genetic alterations of the *SMARCB1* locus. The upper panel shows PCR for the promoter region of *SMARCB1*. Hypermethylation of the CpG islands in MRT-12 and MRT-14 is shown in the lower panel. CpG islands are marked by asterisks. The bottom panel shows normal control.

Table 1. Mutations⁄methylations of *SMARCB1* (*SNF5/INI1*) in malignant rhabdoid tumor (MRT)

Sample name	Attribute	22q	Mutation⁄methylation of *SMARCB1*
KYM-1	Cell line	homoD	homoD
TM87-16	Cell line	homoD	homoD
TTC-1240	Cell line	UPD	G646T (E216 stop)
TTC-549	Cell line	homoD	homoD
TTC-642	Cell line	UPD	C118T (R40 stop)
TTN-45	Cell line	UPD + homoD	homoD
YAMRT	Cell line	UPD	del exons 1–3
STM-91-01	Cell line	homoD	homoD
RTK(J)-4N	Cell line	homoD	homoD
MRT-2	Primary	homoD	homoD
MRT-3	Primary	homoD	homoD
MRT-4	Primary	homoD	homoD
MRT-5	Primary	UPD + homoD	homoD
MRT-6	Primary	UPD + homoD	homoD
MRT-7	Primary	heteroD	G646T (E215 stop)
MRT-8	Primary	UPD + homoD	homoD
MRT-9	Primary	UPD	27 bp to exon 6 553 del
MRT-10	Primary	Normal	
MRT-12	Primary	heteroD	Methylation
MRT-13	Primary	heteroD	ag to aa intron 5, D224 stop
MRT-14	Primary	heteroD	Methylation

del, deletion; heteroD, heterozygous deletion; homoD, homozygous deletion; UPD, uniparental disomy.

PRPTD (Table 2).[18,21,22] Detection of homozygous deletions was also of interest because they provide an important clue to pinpoint tumor suppressor loci. In fact, *SMARCB1* was identified from homozygously deleted regions at 22q11.2.[4] Of note, we found a homozygous deletion of the *CNTNAP2* locus at 7q35–q36 in one specimen (STM-91-01), and another two cases (TTC-549 and MRT-7) showed a hemizygous deletion in this region (Fig. 2a). The commonly deleted region of the *CNTNAP2* locus was expanded in a 534-kb region (ch7:146,183,963-146,718-030) at 7q35–q36, and a homozy-

gous deletion was involved in only exons 9–10 of *CNTNAP2*. Unfortunately, we were not able to completely exclude the possibility that this may represent copy number variations (CNV) rather than real homozygous⁄hemizygous deletions, because these homozygous deletions were found in established MRT cell lines. However, in our SNP array database, we did not find any CNV at the *CNTNAP2* locus in 100 normal samples, but hemizygous⁄homozygous deletions were observed in two neuroblastoma cell lines (NB-16 and NB-19) (data not shown), suggesting that this deletions would be somatic events rather than CNV. Complete or incomplete losses of genetic materials at seven loci were confirmed by quantitative genomic PCR (Fig. S1).

***CNTNAP2* aberrations found in MRT.** *CNTNAP2* was a single gene found in a novel recurrent homozygous deletion at 7q35–q36. Thus, to assess the involvement of *CNTNAP2* in MRT pathogenesis, mutation, expression, and methylation analyses were carried out in our series. Through mutation analysis of the coding region of *CNTNAP2*, we found a novel R157C missense mutation in a fresh tumor of MRT, which was not found in 60 healthy volunteers and not registered in the dbSNP 137 (http://www.ncbi.nlm.nih.gov/projects/SNP/snp_summary.cgi?view+summary=view+summary&build_id=137) or 1000 Genomes (http://www.1000genomes.org/) databases (Fig. 2b). This single nucleotide change was scored as "probably damaging" or "damaging" by two computational prediction software packages, SIFT (http://sift.jcvi.org/) and PolyPhen-2 (http://genetics.bwh.harvard.edu/pph2/). *CNTNAP2* expression was not detected in three of nine cell lines by RT-PCR (Fig. 2b). Because a homozygous deletion in *CNTNAP2* detected in STM-91-01 cells was partial and limited within exons 9–10, the transcript of exons 2–4 of STM-91-01 was detected, although this specimen had a homozygous deletion (Fig. 1b).

In addition, these three cell lines lacking *CNTNAP2* expression displayed complete or partial methylation of the CpG island of *CNTNAP2* (Fig. 2b,c). Methylation analysis was also carried out in 20 neuroblastoma cell lines, but we did not detect any methylation of CpG islands of *CNTNAP2* (data not shown). To elucidate whether hypermethylation of *CNTNAP2* blocked gene expression in MRT cells, we subjected all three

Table 2. Recurrent chromosomal gains and losses in malignant rhabdoid tumor

Chromosome	Position†		Length (kb)	No. of affected samples	Gene(s)
	Start	End			
Gain					
1	120 804 640	245 519 990	124 715	Four (CL: TM87-16, TTC-549, YAMRT; P: MRT-8)	Many genes
2	41 745 732	42 067 857	322	One (CL: TTC1240)	None
3	158 297 982	158 507 647	209	Two (CL: TM87-16; P: MRT-8)	*CCNL1, VEPH1*
7	123 981 822	124 568 564	587	Four (CL: TM87-16, TTC-1240, TTC-549, TTN-45)	*POT1*
7	125 675 684	125 906 795	231	Two (CL: TM87-16, KYM-1)	*GRM8*
7	130 358 924	130 939 457	580	Three (CL: TM87-16, TTC-1240, TTN-45)	None
16	76 268 665	77 096 360	828	Two (CL: TM87-16, KYM-1)	*CLEC3A, WWOX*
Loss					
2	140 875 055	141 241 576	366	One (CL: STM-91-01)	*LRP1B*
3	60 099 620	60 538 672	439	Three (CL: TM87-16, TTC-642, YAMRT)	*FHIT*
3	78 740 688	78 995 893	255	Two (CL: TM87-16; P: MRT-8)	*ROBO1*
4	182 649 464	182 977 255	328	Three (CL: TTC-642, KYM-1, RTK(J)-4N)	None
7	69 446 093	69 593 327	147	Two (CL: TM87-16, TTC-642)	*AUTS2*
7	146 183 963	146 718 030	534	Three (CL: STM-91-01, TTC-549; P: MRT-7)	*CNTNAP2*
9	9 582 260	10 072 420	490	Three (CL: TM87-16, TTC-1240, KYM-1)	*PTPRD*
16	71 464 505	71 708 905	244	Two (CL: TTC-642; P: MRT-8)	*ATBF1*

†NCBI build 35. List of lesions detected in more than two cases, and known genes in the regions. CL, cell line; P, primary sample.
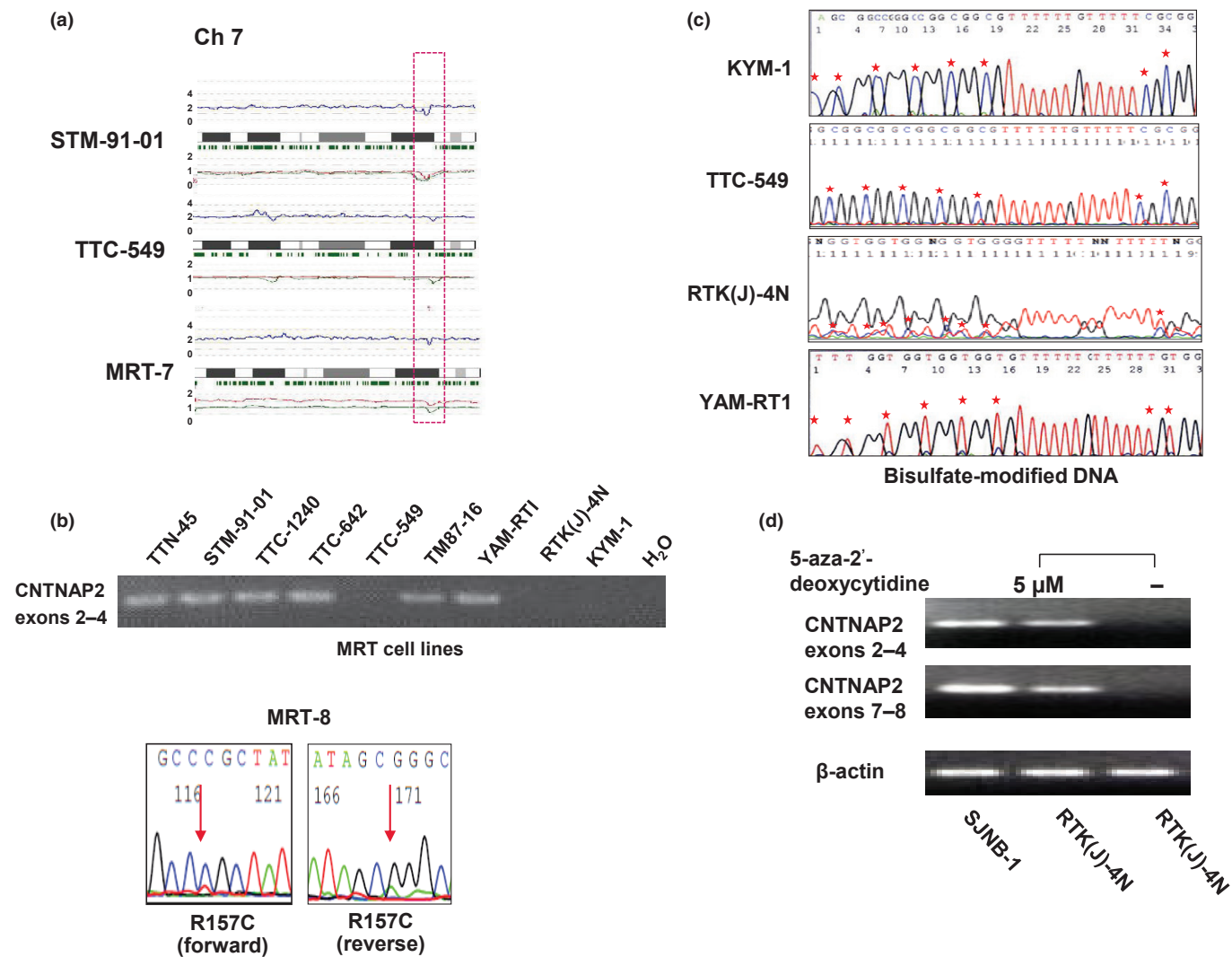
Fig. 2. Recurrent deletions of chromosome 7q35–q36 and *CNTNAP2* alterations in malignant rhabdoid tumor (MRT). (a) Deletions of chromosome 7q35–q36 in three specimens detected by single nucleotide polymorphism (SNP) array. For each panel, total copy numbers (tCNs; red dots), moving averages of tCNs for five consecutive SNPs (blue line), an ideogram of the relevant chromosome, location of heterozygous SNP calls (green bars), and allele-specific copy numbers (AsCNs) averaged for five consecutive SNPs (red and green lines for larger and smaller alleles, respectively) are plotted. (b) Expression and mutation analyses of MRT. Upper panel shows RT-PCR analysis of *CNTNAP2* in nine cell lines. Sequence chromatogram of R157C missense mutation detected in a fresh tumor, MRT-8, is shown in the lower panel. (c) Bisulfate modification- and methylation-specific PCR for *CNTNAP2* in cell lines. Hypermethylation of CpG islands in KYM-1, TTC-549, and RTK(J)-4N cell lines is shown in the upper panel. The lower panel shows control. CpG islands are marked by asterisks. (d) Representative results of re-expression of transcriptionally silenced *CNTNAP2* after treatment with 5-aza-deoxycytidine in MRT cell lines. Reverse transcription-PCR analysis of KYM-1 cell line harvested following 72 h of incubation with control media (−) and 5 μM 5-aza-2-deoxycytidine (+). SJNB-1 neuroblastoma cell line, which expressed abundant *CNTNAP2*, was used as a positive control.

cell lines to 3 days' exposure to 5-aza-deoxycytidine. As shown in Figure 2(d), *CNTNAP2* expression was induced by 5-aza-deoxycytidine treatment in the three cell lines, indicating that methylation of the CpG island is a direct mechanism for *CNTNAP2* silencing in MRT.

Discussion

Our SNP-chip analysis revealed a high frequency of deletion at 22q11.2 in the MRT genome, indicating the unique patterns in the genome imbalance map that characterizes MRT.[10] In our analysis, most MRT specimens showed biallelic genetic aberrations of *SMARCB1,* but three cases did not show biallelic genetic abnormalities of *SMARCB1.* Among them, two cases with kidney MRT showed heterozygous deletions of the

22q11.2 locus and complete methylation of the promoter region of *SMARCB1*, suggesting that not only genetic events, but also epigenetic changes contributed to biallelic inactivation of *SMARCB1* in MRT. Although epigenetic silencing of *SMARCB1* in MRT has never been reported, epigenetic alterations of promoter regions of *SMARCB1* should be considered for the possible alterations for inactivation of *SMARCB1* in MRT.

In previous reports, heterozygous knockout mice developed tumors consistent with MRT,[23] beginning as early as 5 weeks of age, but mice crossed with SMARCB1^{+/−} and CCND1^{−/−} mice did not develop any spontaneous tumor.[23] Thus, these findings suggest that CCND1, located at 11q13.3, may be a key mediator involved in the genesis of MRT. Of interest, our analysis identified recurrent gains at CCNL1, which functions in association with cyclin-dependent kinases, including

CCND1, suggesting that CCNL1 acts as one of the mediators involved in the development of MRT. We also found recurrent losses at the *PTPRD* locus on 9p23 and gains at the *POT1* locus on 7q31. *PTPRD* and *POT1* have been shown to be mutated or downregulated in several human cancers, including neuroblastoma, lung cancer, and chronic myeloid leukemia;[22,24,25] thus, further analysis of these gene alterations in a large number of MRT samples would be necessary to assess their involvement in the pathogenesis of MRT.

The *CNTNAP2* gene encodes a single-pass transmembrane protein, mediating cell–cell interactions in the CNS and/or peripheral nervous system.[26] This gene is located in a common fragile site that is inactivated in different types of cancers, including brain tumor, ovarian cancer, and breast cancer.[27] Recently, CNTNAP2 was shown to be translocated and methylated in a subset of glioma and demonstrated functional characteristics of a tumor suppressor gene.[28] In our analysis, recurrent homozygous/hemizygous deletions involving the *CNTNAP2* locus were newly identified, and expression of *CNTNAP2* was substantially reduced in 33% of MRT cell lines, supporting the fact that *CNTNAP2* is a putative second tumor suppressor gene for MRT. Furthermore, methylation of the promoter region of *CNTNAP2* has been reported in not only glioma, but also in pancreatic adenocarcinoma.[18] In accordance with this, two cell lines, KYM-1 and TTC-549, showed complete methylation of *CNTNAP2* resulting in loss of CNTNAP2 expression. However, one cell line, RTK(J)-4N, displayed partial methylation of the CpG island, although *CNTNAP2* expression was absent in this cell line. Therefore, additional mechanisms, such as mutations of the promoter region of *CNTNAP2* in the unmethylated allele, would also be associated with silencing of *CNTNAP2* in RTK(J)-4N. Because a corresponding normal sample of the MRT-8 case with *CNTNAP2* R157C mutation was not available, we could not exclude the possibility that this mutation would be a rare SNP. However, the mutant allele was relatively low compared to the wild-type allele, suggesting that the single nucleotide change detected at R157 in MRT-8 was most likely to be a somatic mutation rather than non-functional SNPs. Taken together, these findings suggested that *CNTNAP2* is a candidate gene target in a subset of MRT.

In conclusion, consistent with other reports, our results illustrate that *SMARCB1* is the primary gene implicated in the pathogenesis of MRT.[10] Although frequencies of recurrent genetic changes other than the *SMARCB1* locus were low, our findings suggest that *CNTNAP2* is one of the potential second gene targets for MRT. To our knowledge, this is the first report to describe aberrations of *CNTNAP2* in MRT. Further studies are necessary to unravel the oncogenic effects of *CNTNAP2* in MRT.

Acknowledgments

Disclosure Statement

The authors have no conflicts of interest.

References

1 Beckwith JB, Palmer NF. Histopathology and prognosis of Wilms tumors: results from the First National Wilms' Tumor Study. *Cancer* 1978; **41**: 1937–48.
2 DeYoung BR, Swanson PE, Argenyi ZB *et al.* CD31 immunoreactivity in mesenchymal neoplasms of the skin and subcutis: report of 145 cases and review of putative immunohistologic markers of endothelial differentiation. *J Cutan Pathol* 1995; **22**: 215–22.
3 Bhattacharjee M, Hicks J, Langford L *et al.* Central nervous system atypical teratoid/rhabdoid tumors of infancy and childhood. *Ultrastruct Pathol* 1997; **21**: 369–78.
4 Versteege I, Sevenet N, Lange J *et al.* Truncating mutations of hSNF5/INI1 in aggressive paediatric cancer. *Nature* 1998; **394**: 203–6.
5 Biegel JA, Fogelgren B, Wainwright LM, Zhou JY, Bevan H, Rorke LB. Germline INI1 mutation in a patient with a central nervous system atypical teratoid tumor and renal rhabdoid tumor. *Genes Chromosom Cancer* 2000; **28**: 31–7.
6 Carter JM, O'Hara C, Dundas G *et al.* Epithelioid malignant peripheral nerve sheath tumor arising in a schwannoma, in a patient with "neuroblastoma-like" schwannomatosis and a novel germline SMARCB1 mutation. *Am J Surg Pathol* 2012; **36**: 154–60.
7 Hulsebos TJ, Plomp AS, Wolterman RA, Robanus-Maandag EC, Baas F, Wesseling P. Germline mutation of INI1/SMARCB1 in familial schwannomatosis. *Am J Hum Genet* 2007; **80**: 805–10.
8 Calderaro J, Moroch J, Pierron G *et al.* SMARCB1/INI1 inactivation in renal medullary carcinoma. *Histopathology* 2012; **61**: 428–35.
9 Chen Y, Takita J, Choi YL *et al.* Oncogenic mutations of ALK kinase in neuroblastoma. *Nature* 2008; **455**: 971–4.
10 Jackson EM, Sievert AJ, Gai X *et al.* Genomic analysis using high-density single nucleotide polymorphism-based oligonucleotide arrays and multiplex ligation-dependent probe amplification provides a comprehensive analysis of INI1/SMARCB1 in malignant rhabdoid tumors. *Clin Cancer Res* 2009; **15**: 1923–30.
11 Fruhwald MC, Hasselblatt M, Wirth S *et al.* Non-linkage of familial rhabdoid tumors to SMARCB1 implies a second locus for the rhabdoid tumor predisposition syndrome. *Pediatr Blood Cancer* 2006; **47**: 273–8.
12 Takita J, Chen Y, Okubo J *et al.* Aberrations of NEGR1 on 1p31 and MYEOV on 11q13 in neuroblastoma. *Cancer Sci* 2011; **102**: 1645–50.
13 Nannya Y, Sanada M, Nakazaki K *et al.* A robust algorithm for copy number detection using high-density oligonucleotide single nucleotide polymorphism genotyping arrays. *Cancer Res* 2005; **65**: 6071–9.
14 Uno K, Takita J, Yokomori K *et al.* Aberrations of the hSNF5/INI1 gene are restricted to malignant rhabdoid tumors or atypical teratoid/rhabdoid tumors in pediatric solid tumors. *Genes Chromosom Cancer* 2002; **34**: 33–41.
15 Zweier C, de Jong EK, Zweier M *et al.* CNTNAP2 and NRXN1 are mutated in autosomal-recessive Pitt-Hopkins-like mental retardation and determine the level of a common synaptic protein in Drosophila. *Am J Hum Genet* 2009; **85**: 655–66.
16 Takita J, Ishii M, Tsutsumi S *et al.* Gene expression profiling and identification of novel prognostic marker genes in neuroblastoma. *Genes Chromosom Cancer* 2004; **40**: 120–32.
17 Takita J, Yang HW, Chen YY *et al.* Allelic imbalance on chromosome 2q and alterations of the caspase 8 gene in neuroblastoma. *Oncogene* 2001; **20**: 4424–32.
18 Omura N, Li CP, Li A *et al.* Genome-wide profiling of methylated promoters in pancreatic adenocarcinoma. *Cancer Biol Ther* 2008; **7**: 1146–56.
19 Takita J, Hayashi Y, Nakajima T *et al.* The p16 (CDKN2A) gene is involved in the growth of neuroblastoma cells and its expression is associated with prognosis of neuroblastoma patients. *Oncogene* 1998; **17**: 3137–43.
20 Hoot AC, Russo P, Judkins AR, Perlman EJ, Biegel JA. Immunohistochemical analysis of hSNF5/INI1 distinguishes renal and extra-renal malignant rhabdoid tumors from other pediatric soft tissue tumors. *Am J Surg Pathol* 2004; **28**: 1485–91.
21 Muller D, Millon R, Theobald S *et al.* Cyclin L1 (CCNL1) gene alterations in human head and neck squamous cell carcinoma. *Br J Cancer* 2006; **94**: 1041–4.
22 Ramsay AJ, Quesada V, Foronda M *et al.* POT1 mutations cause telomere dysfunction in chronic lymphocytic leukemia. *Nat Genet* 2013; **45**: 526–30.

23 Tsikitis M, Zhang Z, Edelman W, Zagzag D, Kalpana GV. Genetic ablation of Cyclin D1 abrogates genesis of rhabdoid tumors resulting from Ini1 loss. *Proc Natl Acad Sci USA* 2005; **102**: 12129–34.

24 Nair P, De Preter K, Vandesompele J, Speleman F, Stallings RL. Aberrant splicing of the PTPRD gene mimics microdeletions identified at this locus in neuroblastomas. *Genes Chromosom Cancer* 2008; **47**: 197–202.

25 Solomon DA, Kim JS, Cronin JC *et al.* Mutational inactivation of PTPRD in glioblastoma multiforme and malignant melanoma. *Cancer Res* 2008; **68**: 10300–6.

26 Poliak S, Gollan L, Martinez R *et al.* Caspr2, a new member of the neurexin superfamily, is localized at the juxtaparanodes of myelinated axons and associates with K+ channels. *Neuron* 1999; **24**: 1037–47.

27 McAvoy S, Ganapathiraju SC, Ducharme-Smith AL *et al.* Non-random inactivation of large common fragile site genes in different cancers. *Cytogenet Genome Res* 2007; **118**: 260–9.

28 Bralten LB, Gravendeel AM, Kloosterhof NK *et al.* The CASPR2 cell adhesion molecule functions as a tumor suppressor gene in glioma. *Oncogene* 2010; **29**: 6138–48.

Supporting Information

Additional supporting information may be found in the online version of this article:

Fig. S1. Quantitative-genomic PCR for chromosomal deleted regions detected by single nucleotide polymorphism-chip analysis in malignant rhabdoid tumor.

Table S1. Analyzed samples of malignant rhabdoid tumor and single nucleotide polymorphism array platform.

Table S2. Primer sets for quantitative-genomic PCR in malignant rhabdoid tumor.